Mining Science, vol. 25, 2018, 71–99

www.miningscience.pwr.edu.pl

Mining Science

(Previously Prace Naukowe Instytutu Gornictwa Politechniki Wroclawskiej, ISSN 0370-0798)

ISSN 2300-9586 (print)
ISSN 2353-5423 (online)

Received March 5, 2018; reviewed; accepted August 2, 2018

USE OF HIGH SPATIAL RESOLUTION SATELLITE DATA FOR MONITORING AND CHARACTERIZATION OF DROUGHT CONDITIONS IN THE NORTHWESTERN ALGERIA

Malika ABBES[1]*, Abderrahmane HAMIMED[1], Aicha LAFRID[2], Habib MAHI[2], Laounia NEHAL[1]

[1] University of Mascara, Research Laboratory on Biological Systems and Geomatics (LRSBG)-Algeria
[2] Centre des Techniques Spatiales (CTS)-Algeria

Abstract: Over the last decades, Algeria has witnessed intense and persistent drought periods characterized by a significant rainfall deficit. The Northwestern Algeria, such as the most south Mediterranean regions, is marked by alternating wet and dry periods and mixing between Atlantic and Mediterranean airs. In a climate context increasingly disturbed by anthropogenic activities, it is essential to analyze the dry episodes at spatial and temporal scales. In order to understand this problem, this work aims to use the potential of Landsat satellite imagery for monitoring drought conditions in the Cheliff watershed in the northwestern Algeria. As known, the behavior of vegetation is strongly related to climate changes. On this basis, a comparison of the variations in the standardized normalized difference vegetation index (NDVI) and those of the drought indices calculated from meteorological data was implemented. In fact, the rainfall series from fifty meteorological stations were analyzed. The standardized precipitation index (SPI) was calculated for the years 1987, 2000, 2006, 2011 and 2015, corresponding to the acquisition dates of Landsat images. Similarly, an extraction of the NDVI values was performed for each meteorological station. The linear regression between SPI and NDVI showed a good correlation. Thus, the obtained results enabled establishing a new drought index based essentially on satellite data. This index represents the advantage for monitoring spatially the drought phenomena and can solve the problem of climatic data lack.

Keywords: *drought, Northwestern Algeria, SPI, NDVI, linear regression, satellite imagery*

Corresponding author: malika-abbes@outlook.fr (M. Abbes)

doi: 10.5277/msc182507

1. INTRODUCTION

The North African regions are likely to suffer the most devastating effects of climatic changes because of their geographical location, low institutional capacity to adapt to rapid environmental changes, low incomes of their population, their greater reliance on climate-sensitive sectors, the bad management of water resources, and especially inadequate government mechanisms (Hamed et al., 2018a).

The climate changes direct effects are expected to affect soil, land cover, and hydrologic systems by increasing temperature, high evapotranspiration potential and great variability of rainfall in terms of timing, form and quantity expressed by increasing frequency of extreme events as foods and droughts (IPCC, TAR, 2001; Bates et al., 2008; Hammouri et al., 2016; Hamed et al., 2018a, b). The less replenishment of surface water will be more obvious in semi-arid and arid regions where most of the predictable impacts are already occurring regardless of climate variability, and climate change is expected only to exacerbate these trends (Hammouri et al., 2016; Hamed et al., 2017). North-African countries (Morocco, Algeria, Tunisia and Libya) are facing numerous environmental challenges related mainly to water scarcity issues, as the major economic sectors, especially agriculture, are extremely vulnerable to current climate sensitivity (Radhouane, 2013; Hamed, 2017; Hamed et al., 2018).

Drought is the most complex and least understood of all natural hazards, affecting several countries including Algeria. It is defined as water deficit during a specific period. This phenomenon has negative impacts on the environmental and socio-economic sectors. Its management requires its continuous monitoring and to make the obtained information available to the concerned organization to take effective measurements and afford feasible programs in order to minimize its negative impacts.

This natural disaster differs from a given region to another in accordance with the climate and the hydrology of the area. Recently, and given the importance of the subject, several studies were implemented dealing with global changes and specifically with the drought phenomena. In fact, according to the World Meteorological Organization (WMO), 1.4 billion people were affected by droughts and 1.3 billion died from direct or indirect causes during the period going from 1967 to 1991. As matter of fact and according to some scenarios of global changes, the occurrence and impact of drought will be unfortunately increasing in the upcoming years (WMO). The study and the understanding of this phenomenon are mainly based on the derivation of the climatic indexes, witch have been developed by many scientists (Palmer, 1965; 1968; Gibbs and Maher, 1967; Shafer and Dezman, 1982; Kogan, 1990; 2002; McKee et al. 1993; Keyantash and Dracup, 2004).

In fact, climatic parameters such as precipitation are used to characterize each drought sequence and evaluate its impact on the environment and the population. Currently, space imagery has become a common tool for studying and monitoring the drought phenomena. This work will be focusing on climate drought in the Cheliff watershed.

The choice of this region frequently affected by drought is justified by the fairly dense meteorological network as compared to the rest of the national territory. In fact, it comprises more than fifty active weather stations. In order to characterize and monitor drought in the Chelif watershed, climate data collected from the fifty weather stations were taken into account. The SPI (McKee, 1993) standardized precipitation index was calculated for each station. This index has the advantage of being computable from a single type of climate data (rainfall).

The SPI is widely used by researchers in the field (Ravi Shah et al., 2015; Jing et al., 2018) but given the difficulty of obtaining climate data, and the frequency of gaps in existing series and the reduced number of weather stations, new methods to understand climate phenomena were proposed. These recent methods are based on spatial data. Satellite images were obtained for free and allowed to obtain continuous information in time and space. In order to understand this problematic, the current work attempts to integrate the potential of satellite imagery (Landsat) into the monitoring of climatic conditions in the Chelif watershed (North-West of Algeria).

This watershed is well-differentiated morphologically, geologically and pedologically, with a rugged topography in the middle and higher Cheliff level and a flat topography in the lower Cheliff level, the elevations range from 40 m in the lower Cheliff level to 1 600 m in the higher Cheliff (Ababou, 2017).

Several spatial indicators can provide information on the water status of the Earth's surface. Vegetation is an excellent indicator that can provide useful information to characterize the severity of the water deficit. In fact, the sensitivity of the vegetation to humidity variations was exploited here based on the normalized index of NDVI vegetation (Sergio et al., 2015).

The comparison of the acquired results along with those obtained from the climatic indexes allowed the implementation of a new drought index based only on spatial data (NDVI). Indeed, some studies, such as those of Kogan (1993; 1997), had already demonstrated the possibility of using remote sensing in the monitoring of drought through the calculation of certain indicators related to the brightness temperature and the index of Standardized vegetation. A complete analysis of drought indices is provided by Wilhite (2005).

2. STUDY AREA DESCRIPTION

The Cheliff watershed is located in the west central part of northern Ageria and covers an area of approximately 47 667 km^2. It is located in longitude between 0° and 3°30″ East and in latitude between 34° and 36° North. It is bounded northward by the Mediterranean, to the west by the Oranais basin, to the south by the high plains and eastward by the Algerian basin (Fig. 1). It takes its source on the limit of the Tell and Sahara in the Saharan Atlas, precislier in the Djebel Amour culminating to 1937 m,

near Aflou region. It begins by flowing from the South to the North, to reach the Mediterranean at Mostaganem region (west of Algeria). This watershed is well-differentiated morphologically, geologically and pedologically, with a rugged topography in the middle and higher Cheliff level and a flat topography in the lower Cheliff level, the elevations range from 40 m in the lower Cheliff level to 1600 m in the higher Cheliff (Ababou et al., 2017; Douaoui et al., 2014). It is a fairly extensive region with a semi-arid climate in the north and arid climate in the south. It is a transitional region between the Mediterranean climatic system in the north and the Saharan in the south and therefore the rainfall does not exceed 500 mm/year. The most important relative humidity values are recorded during the winter season and the lowest values during the summer season. The average monthly relative humidity (1970–2004) varies between 46% for the month of July and 80% for the two months of January and December (Sabri and Medjerab, 2012).

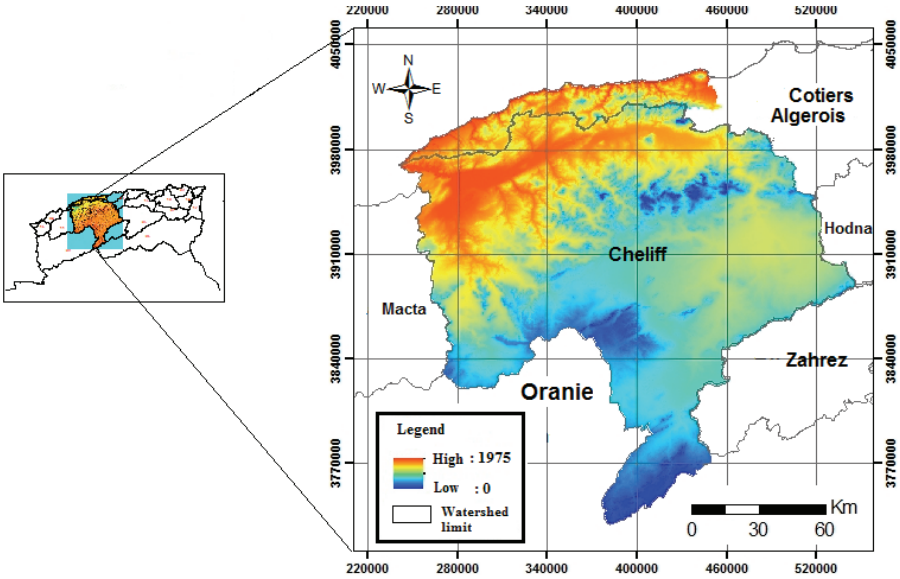

Fig. 1. Geographical situation of the Cheliff watershed

3. DATA SOURCES

3.1. CLIMATE DATA

The drought study in the Cheliff watershed was based on the use of precipitation data coming from 54 meteorological (ONM) and hydrological (ANRH) stations. It is important to note that the rainfall recording period exceeded 30 years in all stations.

The map illustrated in Fig. 2 shows the spatial distribution of rainfall stations and the relief of the studied area. The observation of this map allowed the determination of the spatial distribution of these stations. As matter of fact, the majority of the stations are located in the centre and especially to the West of the studied area. In contrary, the lower zone of the coast, the high plains to the south and the regions of Djelfa and Aflou, are not well covered by the meteorological network.

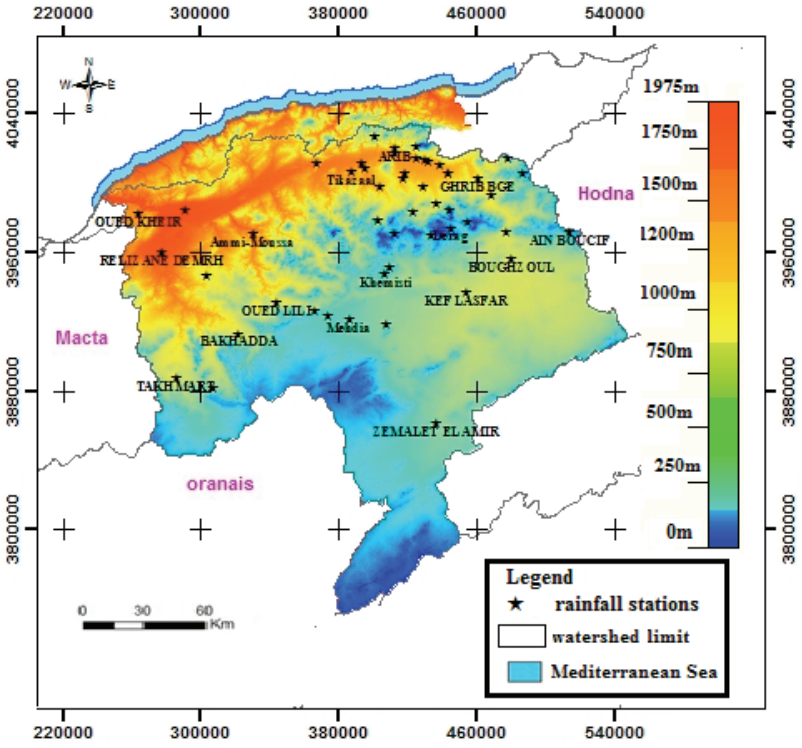

Fig. 2. Spatial distribution of the rainfall stations

3.2. REMOTE SENSING DATA USED

In this study, the obtained satellite images from TM (LANDSAT 5), ETM + (LANDSAT 7) and OLI (LANDSAT 8), were used to achieve our goal. Twenty scenes taken during the periods of 1987-2000-2006-2011 and 2015 were acquired for free from the USGS website. The coverage of the studied area was ensured by a mosaic of 4 scenes. This complicated the choice of images during the download especially by adding other conditions such as vegetation and air humidity which negatively affect the quality of satellite imagery and the date of shooting (which must belong to

the growing season) with a minor percentage of cloud. An overall description of the images used in this current paper is presented in Table 1.

Table 1. Characteristics of the used Landsat images

Satellite	Path	Row	Date
Landsat 5	196	035	1987-09-09
	196	036	1987-09-09
	197	035	1987-10-02
	197	*036*	1987-10-02
	196	035	2011-10-13
	196	036	2011-10-13
	197	035	2011-10-20
	197	*036*	2011-10-20
Landsat 7	196	035	2000-10-06
	196	036	2001-01-10
	197	035	2000-11-30
	197	*036*	2000-11-30
	196	035	2006-10-23
	196	036	2006-10-23
	197	035	2006-10-30
	197	036	2006-10-30
Landsat 8	196	036	2015-11-09
	197	035	2015-10-31
	196	035	2015-11-09
	197	036	2015-10-09

4. METHODOLOGY AND DATA PROCESSING

In this work two approaches were been applied to study the drought in the Cheliff watershed:

- The study of the drought based on the standardized precipitation index “SPI” computed at the base of rainfall stations data provided by the National Hydrous Resources Agency “ANRH” and the National Office Meteos “ONM”.
- The study of drought using high resolution spatial data “Landsat” downloaded from USGS site by calculating the satellite indexes: Standardized Difference Vegetation Index “NDVI”, Vegetation Condition Index “VCI”, Shine temperature Index of “TCI”, Vegetation Health Index “VHI” and finally a correlation between the SPI and NDVI results was performed by linear regression.

4.1. CLIMATE DATA PROCESSING

The analysis of the observation data requires a careful control and verification. Thus, the first goal of this work was to collect all the available rainfall data as well as relevant information related to the study area. Some of the selected stations had gaps that were corrected by calculating the mean arithmetic value of ten years. This method is generally used when there are no well correlated stations with the studied series. This choice was induced by the distance between the selected stations which are poorly correlated with each other. This method can be accepted if missing data are not important (Ketrouci, 2002).

After correcting the basic file and filling the gaps (Table 2), we proceeded to the study of the homogeneity of the data by applying the Wilcoxon test. It consisted of a non-parametric test which uses the series of ranks of the observations instead of the series of values. The Wilcoxon test is based on the following principle: If the sample X comes from the same population as the sample Y, the sample X and Y (union of X and Y) is also derived from this same population (Khaldi, 2005). The results obtained from this test indicated that all the stations were homogeneous.

Table 2. The stations filled

Stations	Year	Month
Sidi Lakhel, Kemenda Ferme, Hachem et Ammi Moussa	1962, 1963, 1965, 1966, 1986, 1987, 1990	September, October, November, December
	1967, 1987	January, February, March, April, May, June, July, August
	2011	October, November, December
Zemalet El Amir, Bougazoul, El Khmis, Toutia, Kaf Lesfer, Médéa Seceur, Pontiba Dam	1987	January, February, March, April, May, June, July, August, September, October, November, December.
Arib Cheliff	1987	November, December, January, February, March, April, May, June, July, August

This was also confirmed by calculating the statistical characteristics of the rainfall series (The average value, standard deviation, median value and coefficient of variability (CV)) as presented in Table 3. The analysis of these results showed the presence of a significant variability in the precipitation rate. It could be related to natural internal processes within the climate system as it is a fairly extended region with a semi-arid climate to the north and arid to the south. This area consists of a transitional region between the Mediterranean climate system in the north and the Saharan one in the south. It is important to mention the presence of regions more watered than others or with variations of the anthropogenic external forcing.

Table 3. Statistical characteristics of the studied rainfall stations

Name of stations	Max.	Min.	Standard deviation	Average	Median	Coefficient of variation
1	**2**	**3**	**4**	**5**	**6**	**7**
Rechiage	649.20	57.30	102.96	248.24	242.27	41.47 %
Sidi boudaoud	274.7	10.60	81.52	121.37	233.60	67.16%
Mehdia	657.80	149.5	109.64	343.16	331.63	31.95%
Ain sebain	653.30	95.4	123.82	331.67	325.98	37.33%
Khemisti	904.7	69.9	177.77	356.11	324.13	49.92%
Layoune	575.6	104.6	95.25	340.88	352.65	27.94 %
Ain boucif	579.46	36.9	156.04	334.26	347.71	46.68%
Kef lasfar	263.80	18.50	65.91	137.60	142.53	47.90%
Boughzoul	414.80	104.7	70.45	277.33	218.5	30.99%
Ksar el boukhari	811.3	164.46	104.80	286.80	262.84	36.54%
Derag	804.44	210.3	142.54	522.19	507.81	27.29%
Zouberia	974.8	230.4	145.65	518.18	504.4	28.10%
Ghrib bge	779.3	237.5	116.07	472.69	472.3	24.45%
Ghrib amont	889.9	211.5	157.21	481.08	473.63	32.67%
Medea secteur	874.1	370.5	140.45	631.11	628.47	22.25%
Domaine feroukhi	610	188.2	99.95	397.84	411.60	25.12%
Ain sultan pep	684.5	209.7	96.93	398.91	392.98	24.29%
Bordj el amir	950	174.1	165.15	380.55	360.09	43.39%
Kherba od hellal	632	51	124.59	327.16	311.56	38.08%
Teniet el had	824	187.51	151.18	527.07	542.38	28.68%
Sidi mokrefi	622199	168.59	101.37	405.75	416.19	24.95%
Tarik ibn ziad	938.30	154.9	152.05	455.68	311.56	33.36%
Arib cheliff	633	194.4	107.30	431.49	444.60	24.86%
Bordj el amir	639.2	241.5	102.60	420.85	422.05	24.38%
El khemis inra	612.9	192.1	87.285	428.11	443.05	20.38%
Sidi lakhdar	733.8	123.3	114.61	304.57	395.55	37.63%
El ababsa	608.7	185.4	82.58	363.38	365.02	22.72%
Elkhemis anrh	691.61	174.29	94.22	426.05	437.76	22.11%
Harreza bge	552.43	176.60	86.87	363.95	348.55	23.87%
Arib ebda	781.1	282	125.40	515.74	527.50	24.31%
Sidi medjehed	1089.3	325	195.80	657.97	633.78	29.75%
El anneb	922.1	303.18	149.45	586.32	582.3	25.48%
El touaibia	594.5	157.50	89.91	313.38	307.05	28.91%
Toutia el hassania	685.90	228.80	103.26	449.43	454.40	22.97%
Rouina mairie	595.5	205.7	80.43	358.11	342.87	22.46%
Rouina mines	445.9	190.8	67.50	329.47	335.4	20.49%
Tikazaal cd 54	533.5	232.3	81.54	359.22	357.45	22.70%
Ponteba dam	696.3	216.3	98.28	412.02	233.6	23.85%

1	2	3	4	5	6	7
Si tayeb	525.30	184.09	76.94	329.73	328.10	23.33%
Ouled abdelkader	792.9	177.6	108.50	351.92	338.57	30.83%
Oued sly	453.90	129.59	299.42	299.42	311.56	27.20%
Sidi hosni	605.3	66.70	110.68	309.22	284.35	35.79%
Oued lili	629.7	163.3	96.11	339.65	318.20	28.29%
Ammi-moussa	676.3	162.8	115.78	366.83	377.98	31.56%
Kenenda fermme	648.5	56.90	136.76	358.50	355.71	38.14%
Sidi-lakhdar	184.79	629.70	85.27	398.58	311.56	21.39%
Bakhadda bge	596.6	172	78.59	315.64	307.15	24.90%
Ain el hadid	561.37	77	100.3	323.49	319.15	31.01%
Takhmart dh1	401	119.8	61.30	245.10	235.37	25.37%
Hacham	499.44	106.5	69.27	240.18	233.6	28.%
Relizane demrh	438.1	161.2	64.99	283.79	292.80	22.90%
Oued kheir	468.9	154.1	83.58	303.26	293.55	27.56%

To better understand this intensity and irregularity, the coefficient of variation was calculated and analysed. It presents a very efficient parameter for measuring the degree of the relative dispersion of particular values around the global average. We noted that the *cv* varies between 20 and 50% for all the stations except that for the station of Sidi Boudaoud which scored a higher value of about 60% a reason for us to reject this station.

4.1.1. CALCULATION OF THE STANDARDIZED PRECIPITATION INDEX "SPI"

The Standardized Precipitation Index (SPI) created by Mckee et al. (1993) is a powerful, flexible to use and simple to compute Index. In fact it only calculates the precipitation parameter. Besides, the SPI index is more effective in analyzing wet periods or cycles than dry periods. To calculate the SPI index, monthly readings of at least 20 to 30 years are required, but preferably over 50 to 60 years or even more, which is the optimal period (Guttman, 1994). This index corresponds to the following formula:

$$SPI = \frac{X_i - X_m}{S_i} \tag{1}$$

where:

Xi: is the cumulative rainfall for a year *i*.

Xm and *Si* are respectively the mean and standard deviation of annual rainfall observed for a given series.

This index actually defines the severity of drought in different classes as presented in Table 4 (Bergaoui and Alouini, 2001; Ardoin-Bardin et al., 2003; Ardoin-Bardin,

2004; Ali and Lebel, 2009; Cheikh et al., 2015). In fact, negative annual values indicate a drought period as compared to the chosen reference period while the positive ones indicate a wet situation.

Table 4. Classification of drought sequences based on SPI

Values of the SPI index	The sequence of drough
2.0 et plus	extremely wet
1.5 to 1.99	very humid
1.0 to 1.49	moderately humid
–0.99 to 0.99	near normal
–1,0 to –1.49	moderately dry
–1.5 to –1.99	very dry
–2 and less	extremely dry

SPI has been used by many authors in different regions in the world (Giddings et al., 2005; Wu et al., 2001; Sönmez et al., 2005; Bodian, 2014). In this work we calculated the annual SPI for all periods and for all stations.

4.2. SATELLITE DATA PROCESSING

The received images must go through an atmospheric treatment called “pre-treatment” which is summed up in the application of the FLAASH module (Fast Line-of-Sight Atmospheric Analysis of Spectral Hyper cubes). It eliminates the influence of gases and aerosols on the signal received by an on-board sensor. Thus, and in order to obtain precise parameters of reflectivity, emissivity, surface temperature and other real physical quantities of surface elements, FLAASH processes only satellite images converted to luminance and calibrated in the appropriate units ($\mu W/(cm^2 \cdot sr \cdot nm)$). For this reason, it was imperative to perform a radiometric calibration.

In order to determine the surface reflectance values at any pixel in the image, an atmospheric correction was applied using FLAASH (Fast Line-of-Sight Atmospheric analysis of Spectral Hyper cubes) correction model implemented in ENVI software. The obtained reflectance values will then be used to calculate the different indices used in this work, such as NDVI, VCI.

We recall that the atmospheric correction is an important step of the pre-processing remotely sensed data which consists to separate the effect of atmospheric constituents from the true surface values, especially the scattering and absorption effects caused by some type of aerosol.

Figure 3 illustrates the quality of the treatment resulting from atmospheric correction by the FLAASH method.

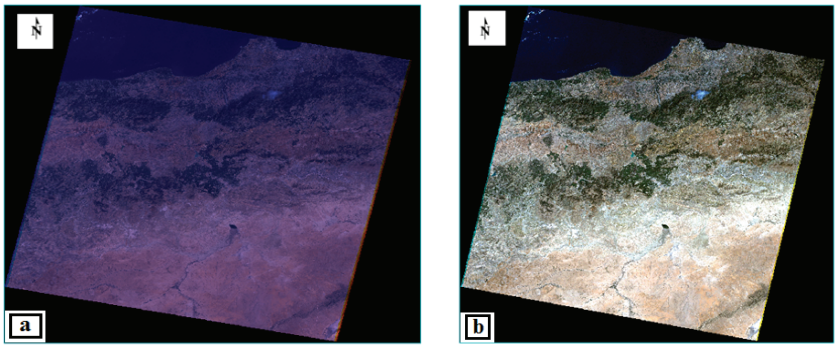

Fig. 3. Result of atmospheric correction by FLAASH: a – before treatment, b – after treatment

4.2.1. SATELLITE INDICES

A) Vegetation Index by Standardized Difference (NDVI)

Among the most popular vegetation indices identified by Richardson and Evert (1992), NDVI is the most widely used in remote sensing (Girard, 2000) and is differencing technique demonstrated the best vegetation change detection (Lyon et al., 1998) It is a standardized difference in vegetation index which is closely correlated with the chlorophyll activity of the plant surfaces and is derived from the difference between the reflectance of near infrared vegetation and that obtained in the red domain divided by their Sum (Michael Hayes, 2007). It is defined as follows:

$$NDVI = \frac{PIR - R}{PIR + R} \tag{2}$$

where:

NDVI: the *NDVI* value of a pixel of the resulting image,

PIR: the numerical value of the same pixel in the near infrared band,

R: the numerical value of the same pixel in the red band.

Values are on a scale of –1 to 1 or the pixel value increases with the presence of vegetation.

Table 5. Classification of the "NDVI" index
(bulletin of engineering geology and the environment (IF: 1972))

NDVI	Classes
<–0.1	water
–0.1 < NDVI < 0.15	bare soils
0.15 < NDVI < 0.25	semi-clear soils
0.25 < NDVI < 0.4	moderately dense vegetation
>0.4	dense vegetation

In Table 5 we present the classification of the NDVI values according to the bulletin of engineering geology and the environment (IF: 1972).

B) Vegetation Condition Index VCI (Kogan, 2003)

This index uses as inputs the minimum, maximum and current NDVI values over several years. It gives information about the conditions of the vegetation during the period of study compared to extreme situations (min and max). The VCI rescales vegetation dynamics between 0 and 100 to reflect relative changes in the moisture condition from extremely bad to optimal (Kogane, 1995; 2003). High VCI values correspond to healthy and unstressed vegetation. It is calculated by the following formula:

$$VCI_{(i)} = \frac{NDVI_{(i)} - NDVI_{(\min)}}{NDVI_{(\max)} - NDVI_{(\min)}} * 100 \tag{3}$$

where:

$NDVI_{(i)}$: *NDVI* of the studied period,

$NDVI_{\min}$: *NDVI* minimum of the studied period,

$NDVI_{\max}$: maximum *NDVI* of the studied period.

The VCI has been used on several continents to detect large-scale drought conditions, and also excessive moisture conditions (Kogan, 1997, 2003; Kogan and al., 2004). Several teams have used the VCI to monitor drought conditions in South Africa (Kogan, 1998), India (Singh et al., 2003) and Greece (Domenikiotos et al. 2004; Kogan et al. 2004). It was also used to derive biomass from pastures in Mongolia or the yield of maize crops in China (Kogan et al., 2004, Kogan et al., 2005, Beaudin and Isabelle, 2007).

C) Brightness Temperature Based Index (TCI)

This indicator is based on the brightness temperature. It is applicable at the regional or continental level, instantaneously or for periods up to a year. TCI also provides useful information on the stress of vegetation due to soil saturation in water (Kogan, 1997; Kogan et al., 2004). The TCI index is calculated as follows:

$$TCI_{(i)} = \frac{T_B^{\max} - T_{B(i)}}{T_B^{\max} - T_B^{\min}} * 100 \tag{4}$$

where:

T_B: gloss temperature,

$T_B^{\min}$: the brightness temperature value,

$T_B^{\max}$: the maximum brightness temperature value.

The low value of TCI indicates to vegetation stress due to severe climatic condition (high temperature) and dryness (Bhuiyan, 2008), compared to the period of study. Concerning the high values, they mainly reflect favourable conditions.

D) Vegetation Condition Index VCI (Kogan, 2003)

This index uses as inputs the minimum, maximum and current NDVI values over several years. It gives information about the conditions of the vegetation during the period of study compared to extreme situations (min and max). The VCI rescales vegetation dynamics between 0 and 100 to reflect relative changes in the moisture condition from extremely bad to optimal (Kogane, 1995; Kogane, 2003). High VCI values correspond to healthy and unstressed vegetation. It is calculated by the following formula:

$$VCI_{(i)} = \frac{NDVI_{(i)} - NDVI_{(\min)}}{NDVI_{(\max)} - NDVI_{(\min)}} * 100 \quad (5)$$

where:

$NDVI_{(i)}$: NDVI of the studied period,

$NDVI_{\min}$: NDVI minimum of the studied period,

$NDVI_{\max}$: maximum NDVI of the studied period.

The VCI has been used on several continents to detect large-scale drought conditions, and also excessive moisture conditions (Kogan, 1997; 2003; Kogan et al., 2004). Several teams have used the VCI to monitor drought conditions in South Africa (Kogan, 1998), India (Singh et al., 2003) and Greece (Domenikiotos et al., 2004) (Kogan et al., 2004). It was also used to derive biomass from pastures in Mongolia or the yield of maize crops in China (Kogan et al., 2004, Kogan et al., 2005, Beaudin and Isabelle, 2007).

E) Vegetation Health Index (VHI)

According to Kogan (1997), temperature condition index "TCI" combined with vegetation condition index "VCI" is a useful source of information about the stress caused to vegetation as a result of drought and has been successfully applied in many different environmental conditions (Kogan et al., 2005; Rojas et al., 2011; Seiler et al., 2007; Unganai and Kogan, 1998; Wu et al., 2013). Combined with field data, these indices appear to be excellent tools for monitoring drought conditions, especially in agriculture. The VHI is defined as follows:

$$VHI = \alpha * VCI + (1 - \alpha) * TCI \quad (6)$$

α being the relative contribution of *VCI* and *TCI* in the *VHI*. According to most publications, $\alpha = 0.5$, assuming the same contribution of the two indices and also due to the lack of more precise information (Kogan, 2000).

5. RESULTS AND DISCUSSION

5.1. SUPERVISED CLASSIFICATION

In the classification process, the supervised classification method was performed using the maximum Likelihood. The latter was based on a set of user-defined classes and training areas. The classes were extracted from the general knowledge obtained from topographic maps and land use. Then, the supervised classification was applied to the images captured during Oct. 1987, Nov. 2000, Sept. 2006, Oct. 2011 and Oct. 2015. Four classes were identified: forest, agriculture, bare soils and water. Figure 5 illustrates the mapping of land use for the studied years.

5.1.1. RESULTS OF SUPERVISED CLASSIFICATION OF SATELLITE IMAGES

Currently, recent studies have shown that the impact of climate change affects the type of vegetation, the nature of the soil ... Sometimes in the positive sense (adaptation of new species with climate and soil ...), sometimes in the direction degradation (Hamed et al., 2010; 2014; 2018b).

The reasons behind the changes that occurred between 1987 and 2011 are presented in Table 6. It is important to note that the total area of study was of 47664 km^2. The area of land use in 1987 shows considerable vegetation cover (Fig. 5). Agriculture occupied an area of 5775.86 km^2, which presents 12% of the territory. The forest extent represented 9740.51 km^2 and bare soils reached 320264.85 km^2.

Table 6. Area of occupancy of the Cheliff watershed

Types of occupations	Area in 1987		Area in 2000		Area in 2006		Area in 2011		Area in 2015	
	km^2	%	km^2	%	km^2	%	km^2	%	km^2	%
Forest	9740.51	20.43	9604.3829	20.14	57771.17	12.10	6098.02	12.79	7050.38	14.79
Agriculture	5775.86	12.11	1598.95	3.35	1370.97	2.87	7115.94	14.92	7931.52	16.64
Water	121.90	0.25	138.50	0.29	84.27	0.17	162.78	0.34	84.03	0.176
Bare soil	320264.8	67.19	36323.02	76.20	40438.41	84.83	34288.09	71.93	32598.91	68.39
Total	47664.85	100	47664.85	100	47664.85	100	47664.85	100	47664.85	100

In 2000, the areas served for agriculture and forests decreased and therefore bare soils expanded. In 2006, there was an important change that affected the forest cover which was reduced by a percentage of 8%. On the other hand, there was a strong increase of bare soils, indicating that the years 2000 to 2006 were affected by a severe drought. As a result, the years 2011 and 2015 witnessed an increase of

agricultural area, reaching 2% for forests covering 13% for agriculture and a decrease of about 16% for bare soils. Land use coverage results are illustrated in Figs. 4 and 5.

There is a highly intimate relationship between the rate of precipitation and the nature of the soil. In highly rainy areas with steep slopes, there will be soil erosion and therefore a total change in the nature of the soil and of course a total change (type of vegetation, evapo-transpiration ...). In moderately rainy areas with medium to low slopes, it will not have a strong change in the nature of the soil (structure and texture) and therefore no significant change in vegetation, evapo-transpiration rate ... (Hamed et al., 2018a, b).

The spatial extent of agricultural land and forests between 1987 and 2000 decreased significantly. The central and western regions were much more affected by this regression and correspond to the wilayas of Tissemsilt and Rélizane areas. On the one hand, bare soils showed a continuous extension. This can be explained by the drought that affected this area during this period. More significant negative changes were recorded during the period going from 2000 to 2006. However, the forest declined by more than 20% of the total area of study to only 12%. While bare soils continued their expansions from 76% to about 85%.

This degradation mainly affected the western part of the Cheliff watershed and was aggravated by the severe drought during that period. On the other hand and between the years 2011 and 2015 there was a significant increase in agriculture and forests and a decrease in the bare soil at the basin level and even much more southward. Generally, the forest degradation is mainly due to a combination of several factors, particularly, natural and anthropogenic. Among the natural factors, we can cite climate change, forest fires, pests and diseases and also land and air pollution. The anthropogenic factors include direct effects of human activities such as; urbanization, over exploitation of wood as well as the criminal fires.

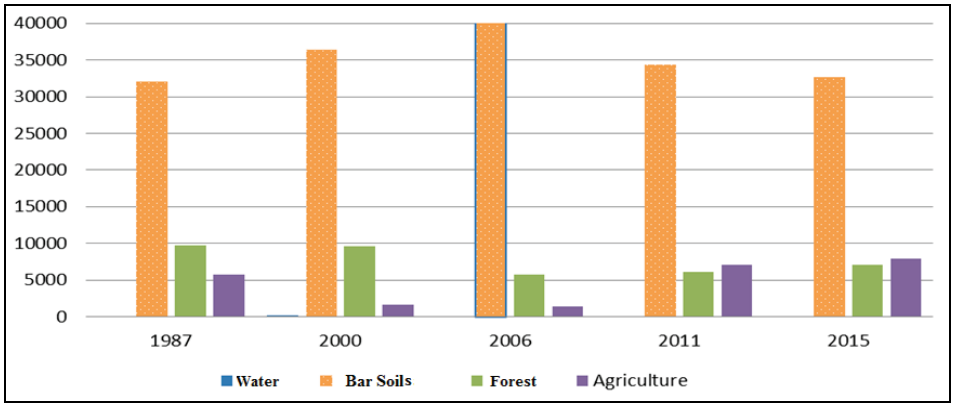

Fig. 4. Soil occupation Areas of the different classes

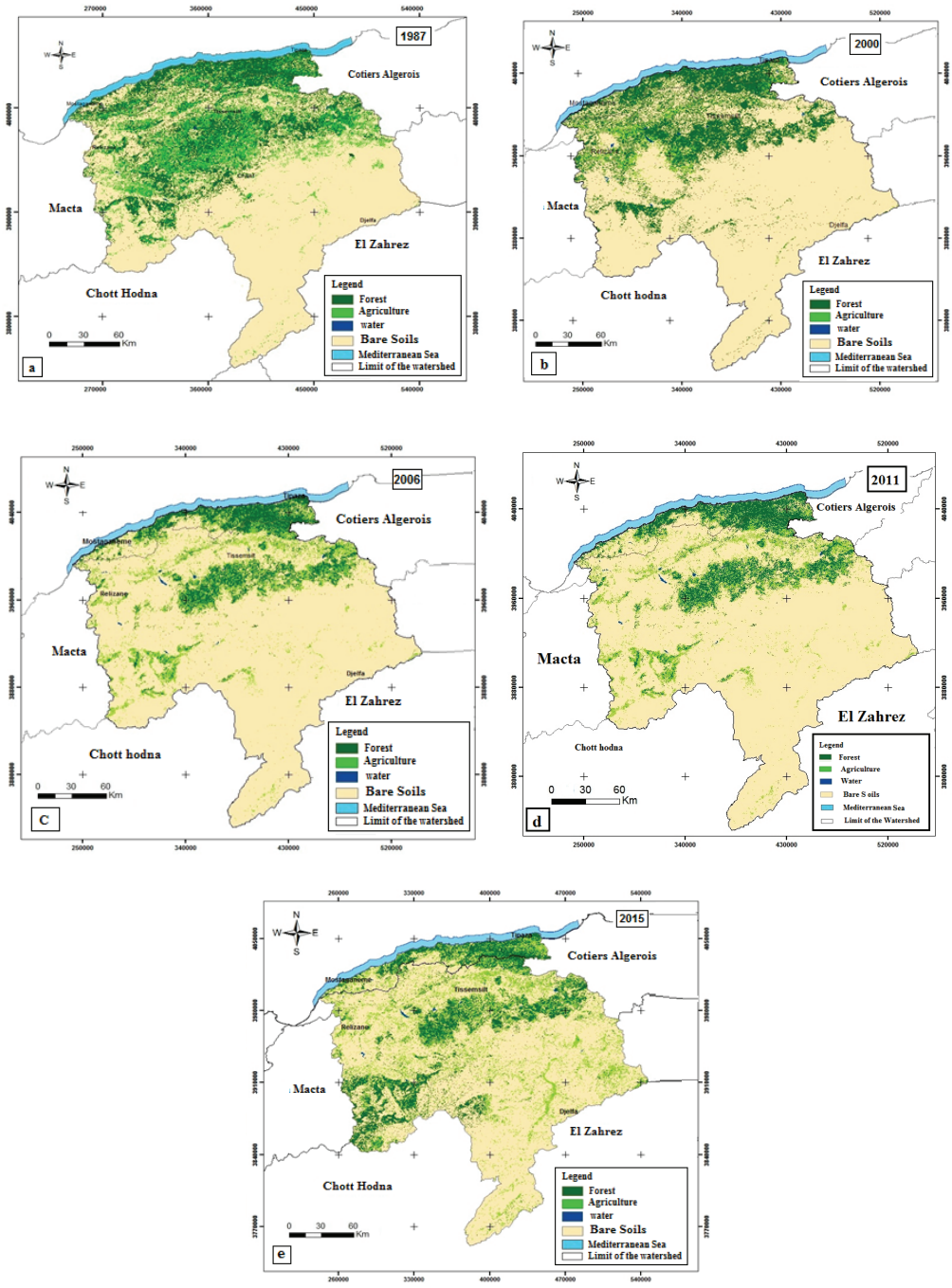

Fig. 5. a–e – Land cover map for the studied period

5.2. SATELLITE DROUGHT INDICES

5.2.1. DERIVATION OF THE NDVI

Table 7 and Fig. 6 shows the change statistics of the NDVI classes, both are of good interest in understanding the change tendency in Vegetation coverage. The *NDVI* value decreased during the period going from 2000 to 2011 for dense vegetation (forests) which diminished from 12.65% to 3.43% and the moderately dense vegetation (agricultural land) which decreased from 15.5 to 9.25%. The low *NDVI* values that indicate bare soils and semi-clear soils increased in frequency.

Table 7. Statistics for the different NDVI classes in 1987, 2000, 2006, and 2015 in the Cheliff watershed

Type of occupancy	Area in 1987		Area in 2000		Area in 2006		Area in 2011		Area in 2015	
	km^2	%	km^2	%	km^2	%	km^2	%	km^2	%
Water	92.39	0.19	160.26	0.33	84.37	0.17	169.71	0.35	181.15	0.38
Bare soils	25982.50	54.51	19982.27	41.92	19466.16	40.83	33281.50	69.82	9517.05	19.96
Semi-clear soils	14070.52	29.51	14100.95	29.58	19071.26	40.01	8156.39	17.11	20775.1	43.58
Moderately dense vegetation	3880.72	8.14	7390.22	15.50	4588.85	9.62	4421.39	9.27	9009.55	18.90
Dense vegetation	3638.69	7.63	6031.12	12.65	4454.18	9.34	1635.83	3.43	8181.56	17.16
Total	47664.84	100	47664.84	100	47664.84	100	47664.84	100	47664.8	100

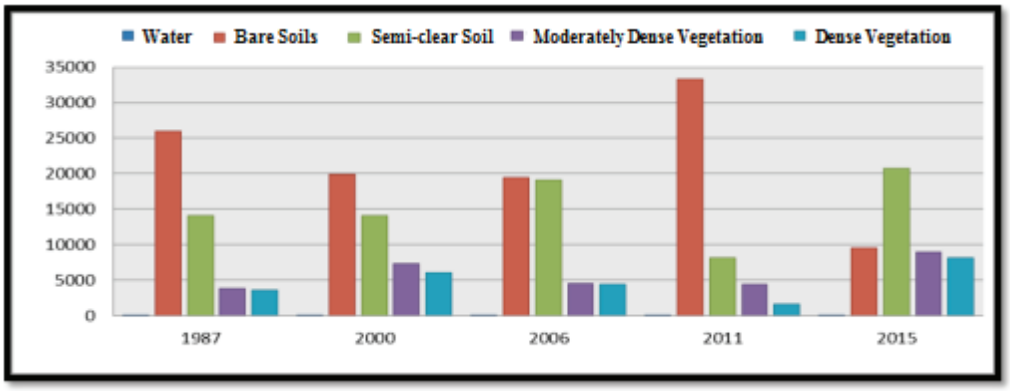

Fig. 6. Areas of different classes of NDVI

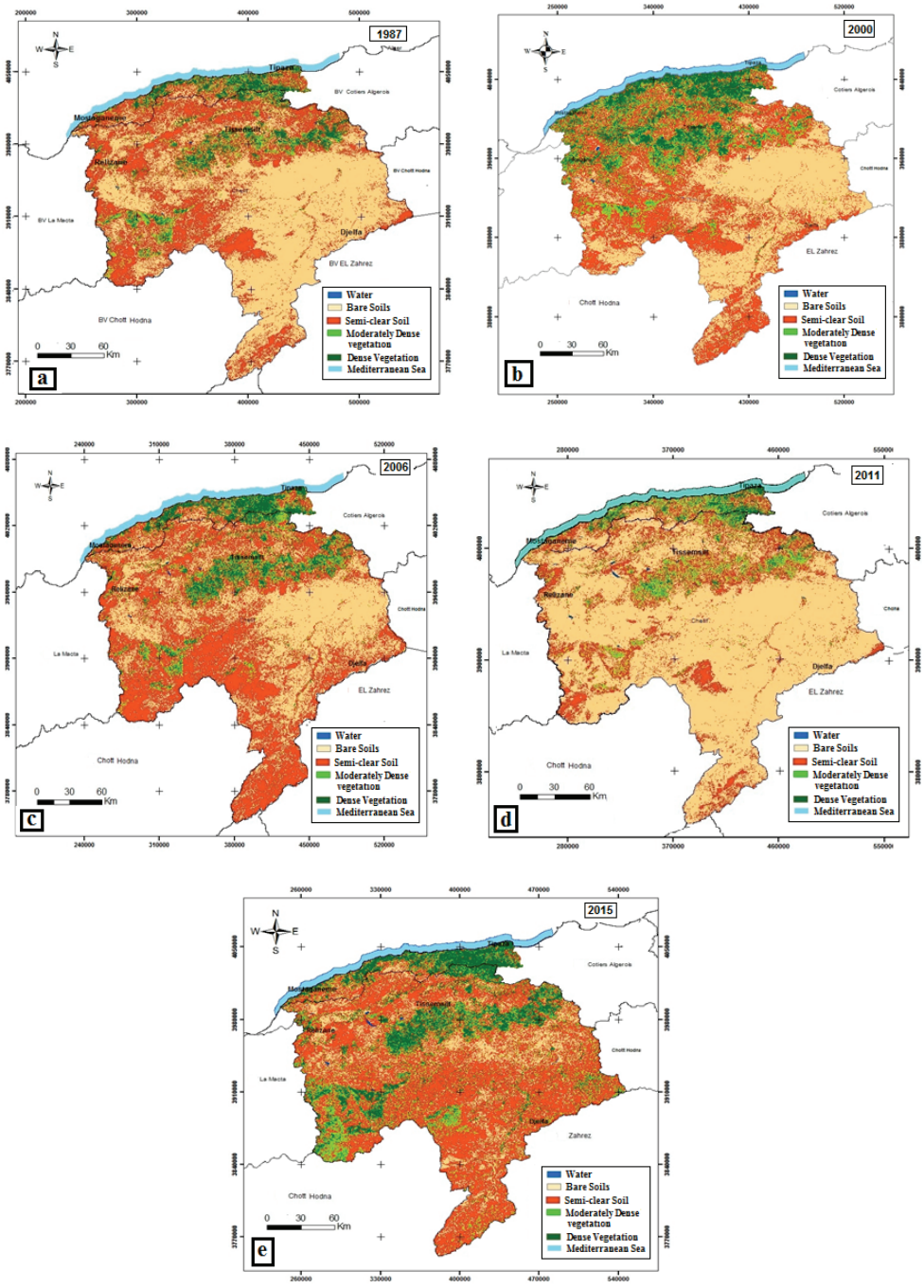

Fig. 7. a–e – maps of the NDVI index for the studied period

The year 2015 witnessed a significant increase of around 14% for the forest class and 9% for the moderately dense vegetation. In order to better understand these observations we proceeded by the NDVI mapping for each year in accordance with the different classes and based on the classification of the (bulletin of engineering geology and the environmental (IF, 1972) as shown in Fig. 7.

5.2.2. DERIVATION OF THE VCI

Special interest has been given to the Derivation of the VCI index since it changes instantaneously in space and time at the ten-day, monthly, seasonal and annual scales, which influence the quantitative and qualitative evaluation of the drought mapping. A geo-processing model under ArcGis's ModelBuilder provided a computerized version of the data (workflow). The compilation results have been integrated in ENVI with the classification function "density slice" and Arcgis according to the universal classification of the VCI. Similarly, the "TCI" and "VHI" indices were calculated to prioritize climate drought.

The VCI image, illustrated in Fig. 8 according to the Kogan et al. classification, indicated is the presence of a high spatial and temporal variability of drought during the years 1987, 2000, 2006, 2011 and 2015. In 1987, drought affected the entire Cheliff Watershed. However, in 2000 the drought has affected the north and extreme southwest of the watershed while the northern and northwestern parts were not affected. In 2006, the drought expanded mainly to the northern part of the region affecting forest cover and agricultural areas. In 2011, the whole territory was totally affected by an extreme drought translating a strong water shortage. Contrarily the year 2015 showed significant values of VCI, which means that there was no drought on the whole watershed during this period.

Once the TCI and VCI indices were derived with a developed Model Builder using ArcGIS 10.1, obtaining the vegetation health index (VHI) became easier (Tucker, C.J. 1983). The obtained results are illustrated in Fig. 9. According to the Kogan and al. (2004) classification (Table 8, we noticed a strong spatio-temporal variability of the drought during the years 1987, 2000, 2006, 2011 and 2015. During 1987, drought affected the entire Cheliff watershed. In 2000, the drought affected the north and the extreme south-west of the Cheliff watershed while the northern and north-western parts were not affected by drought. In 2006, the drought was registered in the northern part of the region and affected the forest cover and agricultural areas. In 2011, the entire territory was totally affected by an extreme drought translating a water shortage. However, in 2015 the VCI values were considerable, which expresses the absence of drought in the whole watershed.

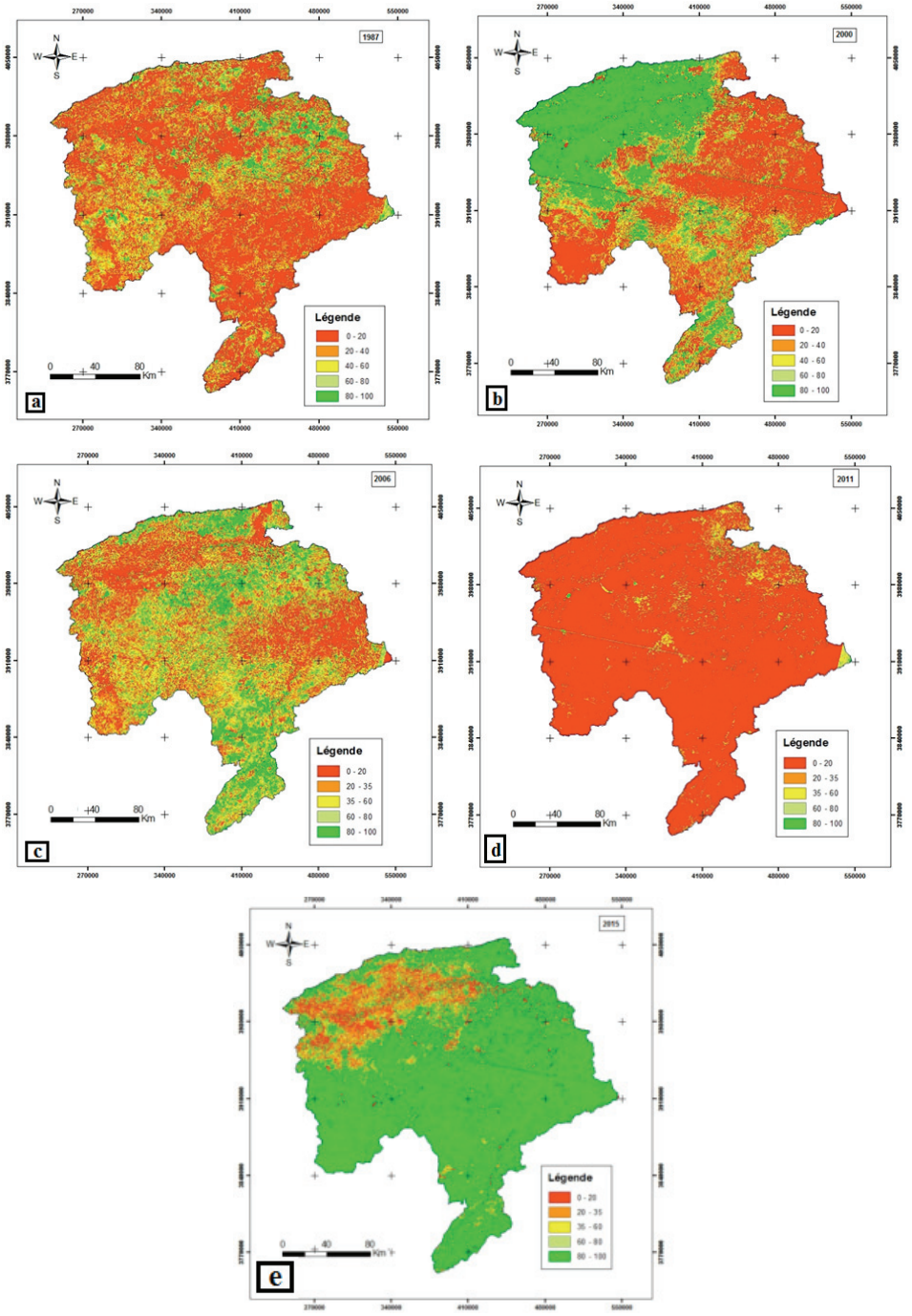

Fig. 8. a–e – Maps of the VCI index during 1987, 2000, 2006, 2011, 2015

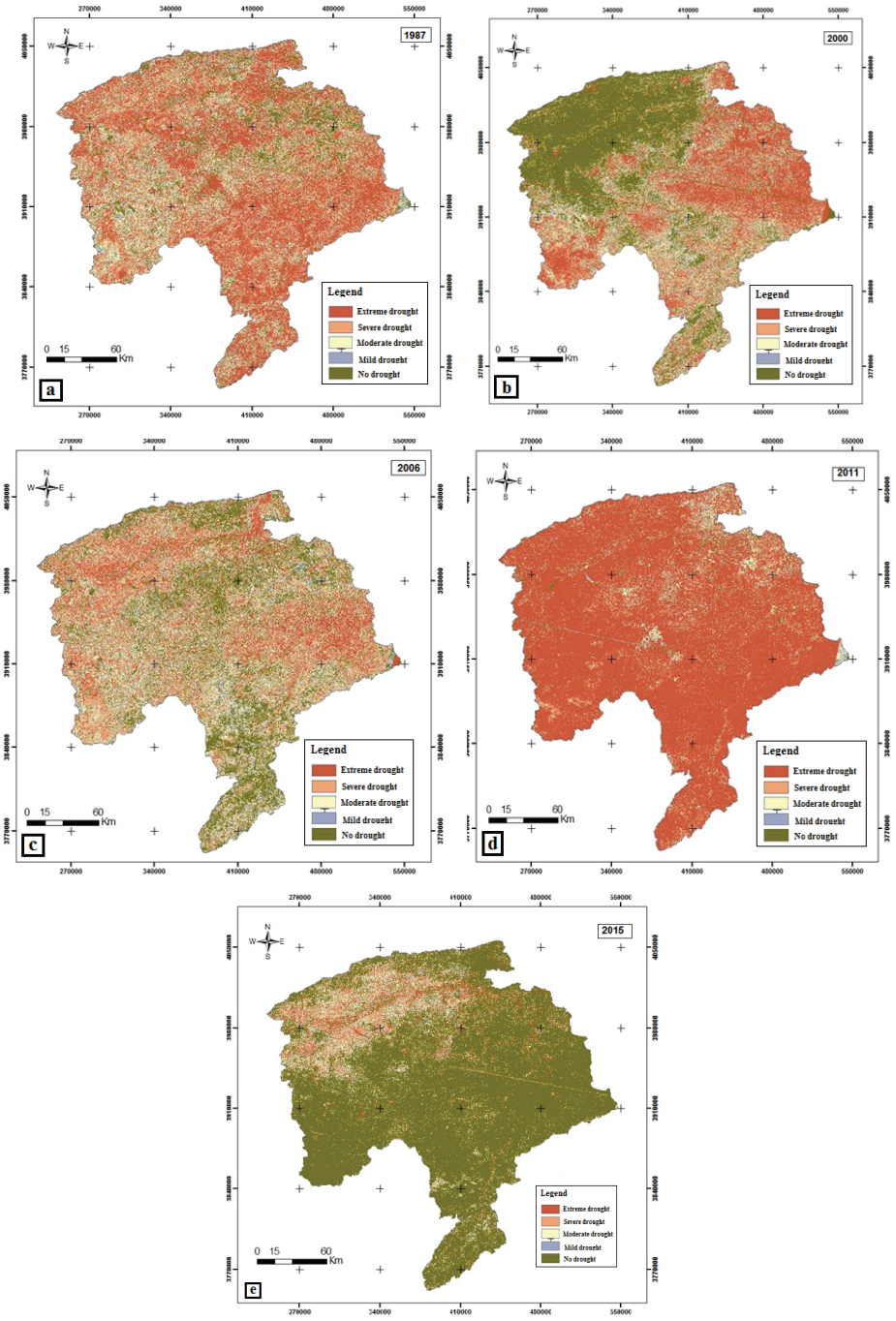

Fig. 9. a–e – VHI index maps for the studied period

5.3. RELATION OF SPI WITH THE NDVI

The relationship between SPI and NDVI was investigated using 50 reference sites. Each site was extracted from the NDVI image and corresponds to an area with 20 km × 20 km around the location of the meteorological stations. The mean, the maximum and the minimum of the NDVI values of each site were used in the linear regression between NDVI and annual SPI, NDVI and mean SPI of two successive years and NDVI and SPI during September.

Before starting the correlation, we extracted, from the NDVI images during different periods, windows corresponding to each meteorological station with a radius of 10 km around these stations. We obtained 50 windows (reference zones) with a grid of 20 × 20 km. For each reference zone we calculated the mean, the maximum and the minimum of the NDVI. These values were subsequently used in the linear regression between NDVI and annual SPI, NDVI and mean SPI of two successive years and NDVI and SPI during September.

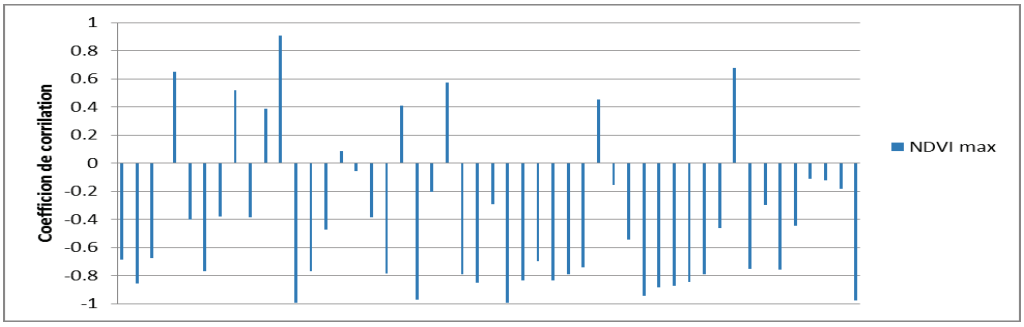

Fig. 10. Correlation between the annual SPI and NDVI min

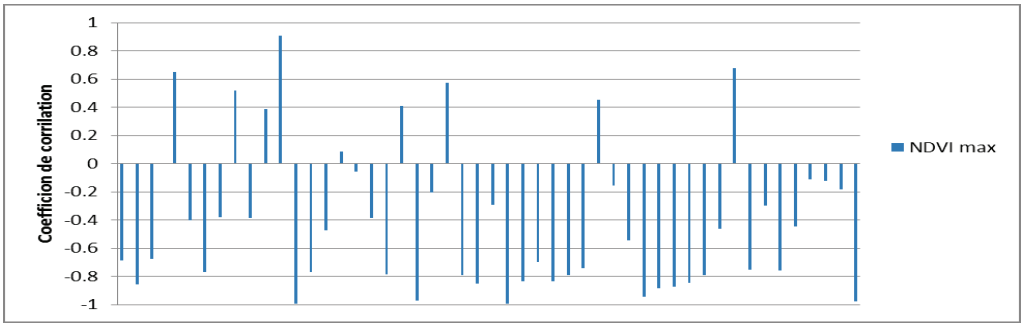

Fig. 11. Correlation result between annual SPI and NDVI max

In Figs. 10 and 11, the number of stations with a correlation coefficient greater than 0.5 correspond to the $NDVI_{max}$ which will be selected to obtain a new SPI index

based on $NDVI_{max}$. The linear regression between annual *SPI* and NDI_{max} is presented in Fig. 12.

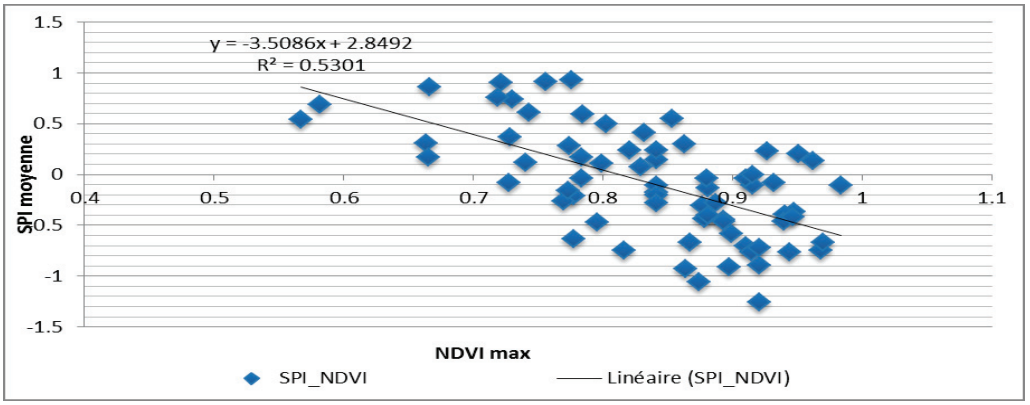

Fig. 12. Linear regression line between NDVI and SPI

We noticed that the maximum of points are condensed around the linear trend curve. The correlation coefficient r is 0.73. This, allowed us to deduce the equation that binds the annual *SPI* and the $NDVI_{max}$:

$$Y = -3.5086X + 2.8492 \tag{6}$$

Consequently:

$$SPI_{NDVI} = -3.5086NDVI_{max} + 2.8492 \tag{7}$$

where:

SPI_{NDVI} is the new drought index based on *NDVI*.

This new *SPI* formula (7) was used to develop new drought index maps based only on *NDVI* data. To validate these results, we compared them with the *SPI* calculated on the basis of meteorological data (Fig. 13).

After mapping the SPI calculated on the basis of the climate data and the SPI_{NDVI}, we noted that there was a strong correlation between the two indices during the 2000, 2006 and 2011. Contrarily, in 1987 there was a big difference especially in the south and north of the region as a result of the large number of gaps in rainfall data for this year.

Since we obtained a very good correlation between the indices for three years out of four, and that the only year that presents an anomaly is due to the lack of data, we can conclude that our results are valid and our proposal for the new SPINDVI index is evident.

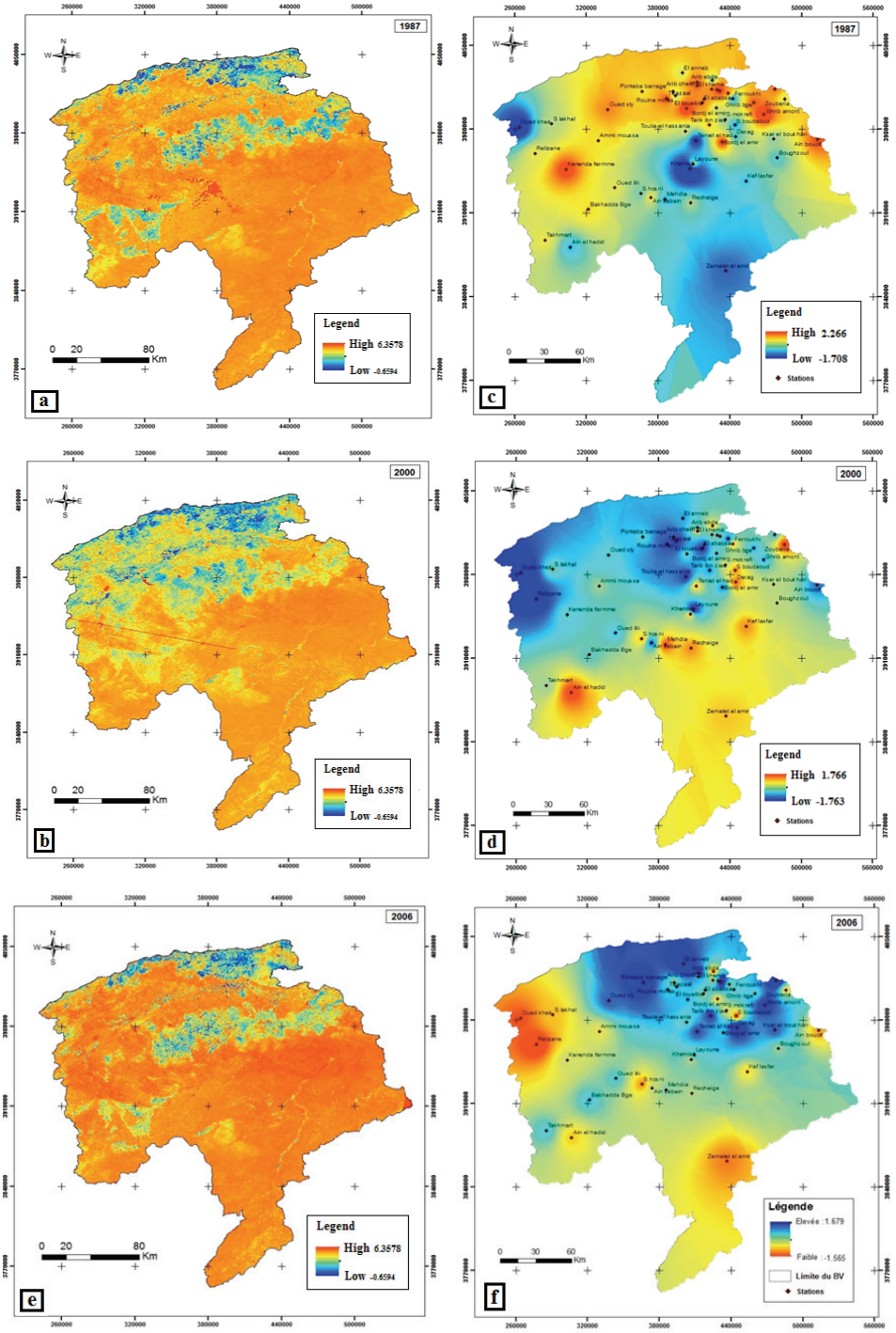
1987
Legend
High 6.3578
Low -0.6594
0 20 80 Km
a
1987
Legend
High 2.266
Low -1.708
Stations
0 30 60 Km
c
2000
Legend
High 6.3578
Low -0.6594
0 20 80 Km
b
2000
Legend
High 1.766
Low -1.763
Stations
0 30 60 Km
d
2006
Legend
High 6.3578
Low -0.6594
0 20 80 Km
e
2006
Légende
Elevée : 1.679
Faible : -1.565
Limite du BV
Stations
0 30 60 Km
f

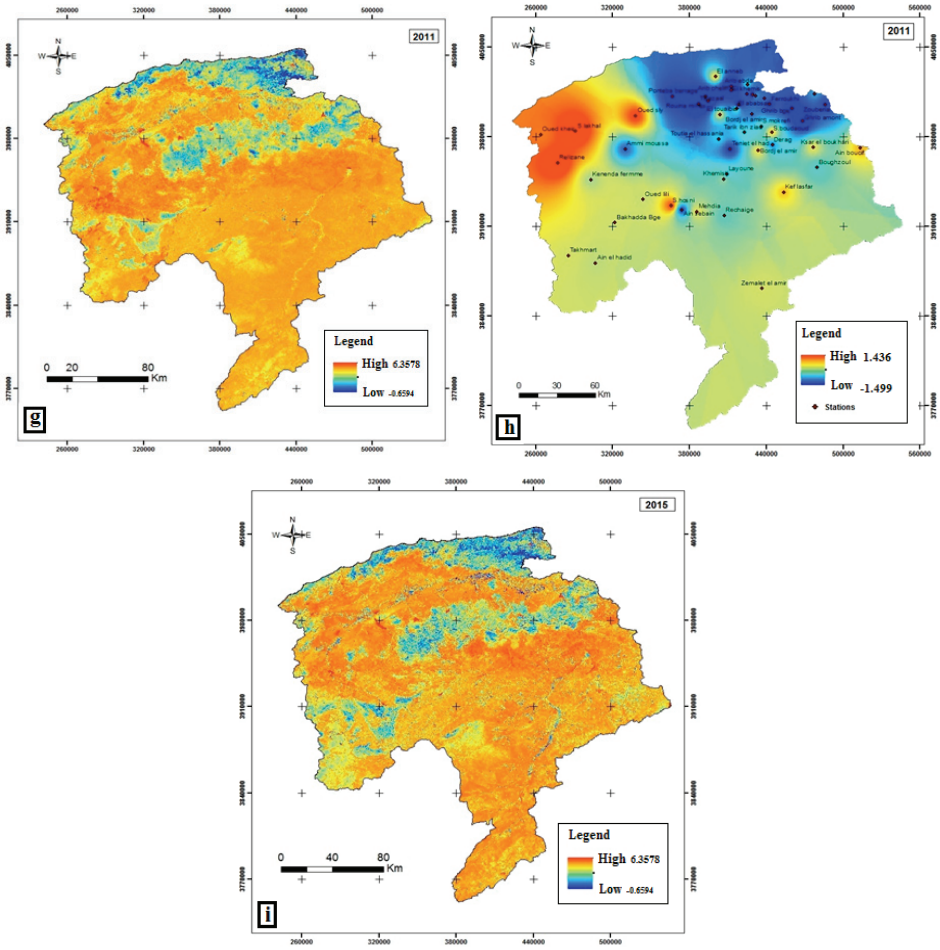

Fig. 13. a, c, e, g, i – maps of the SPI_{NDVI}
and b, d, f, h – maps of climatic indices during the different studied periods

6. CONCLUSION

Our work consisted in presenting the problematic and quoting the indicators that define the drought phenomena. Further, the methodology for determining meteorological and satellite indicators was developed using specific software. Drought is a natural phenomenon that unfavourably affects, directly or indirectly, several areas and sectors such as agriculture, health, environment, socio-economy, and even natural reserves and resources.

The spatial variable that is directly related to soil moisture variation is vegetation. Thus, the drought monitoring was implemented based on the study of plant behaviour

in relation to water stress. This was possible by using the NDVI vegetation index. The latter was used for the calculation of two drought indices, the VCI and VHI, as well as for the calculation of our new SPINDVI index resulting from the comparison between NDVI and SPI.

The obtained results from satellite images were encouraging to study the phenomenon of drought. They were reliable for determining the level of pixel-by-pixel drought. This spatial data was available and easily accessible by comparing it with meteorological data. It should also be noted that the processing time of these satellite data was insignificant compared to the weather data processing time with a minimal margin of error.

The study of drought through the use of remote sensing allowed us to gain a lot of time and obtain more accurate spatial results. This does not preclude pointing out certain limitations regarding the space tool and its products. The multi date presents a problem for the gray level or the reflectance of the images, which introduces noise resulting in radiometric value shifts. In addition, the studied period was a period of low plant density, which poses a problem for the calculation of NDVI.

The integration of remote sensing data and application of GIS provides a powerful tool for efficient watershed management. Indeed, remote sensing data was quite useful for the detection of land use/ land cover in the watershed. For future studies, we recommend researchers to introduce satellite data in order to refine the results and to better understand and predict the phenomenon of climate drought the use of more number of observations and the integration of highly remote sensing data spatial resolution to increase the accuracy of our results.

ACKNOWLEDGEMENTS

We thank ANRH, National Hydric Resource Agency and Centre des Techniques Spatiales (CTS) – Algeria for providing dispersion data for this study. We also thank the editor and the anonymous reviewers for helping improve the quality of our manuscript.

REFERENCES

ABABOU A., BOUTHIBA AEK., CHOUIEB M., REGUIEG YSSAAD H.A., 2017, *Drought Assessment and Rainfall Trend Analysis in a Southern Mediterranean Watershed During the Last Century (1914–2011).*

ABH, 1970–2015, *Data Provided by the Water Basin Agency.*

ANRH, 1970–2015, *Data Provided by the National Hydric Resource Agency.*

BATES B., KUNDZEWICZ Z., WU S., 2008, *Climate Change and Water. Intergovernmental Panel on Climate Change Secretariat*.

BEAUDIN I., 2007, *Potential of Remote Sensing for the Monitoring and Characterization of Drought Conditions in the Mediterranean Environment*, Master's Report in Geomatic Sciences.

BHUIYAN C., 2008, *Desert Vegetation During Droughts: Response and Sensitivity*, Int. Arch. Photogramm. Remote Sens. Spat. Inf. Sci., 37, 907–912.

DASH P., GÖTTSCHE F.M., OLESEN F.S., FISCHER H., 2002, *Land Surface Temperature and Emissivity Estimation from Passive Sensor Data: Theory and Practice – Current Trends*, Int. J. Remote Sens., 23, 2563–2594.

DOUAOUI A., HARKAT S., BOUKHAROUBA K., 2014, *Multi-Site Modeling and Prediction of Annual and Monthly Precipitation in the Watershed of Cheliff (Algeria).*

EDER U., WIECHERT R., SAUER G., 1971, German Patent, DE 2 014 757, 7 October.

FINCKH L., 1924, *Erlauterungen zur Geologische Karte von Preussen, Blatt Charlottenbrunn*, Kgl. Preuss. Geol. L.A. Berlin.

GIBBS W.J., MAHER J.V., 1967, *Rainfall Deciles as Drought Indicators*, Bureau of Meteorology Bulletin, No. 48, Commonwealth of Australia, Melbourne.

Guttman N.B., 1994, *On the Sensitivity of Sample L Moments to Sample Size*, Journal of Climate, 7 (6), 1026–1029.

HAMED Y., 2004, *Caractérisation Hydrogéologique, Hydrochimique et Isotopique des Eaux Souterraines de la Région du Kef (Nord-Ouest Tunisien)*, Mémoire DEA, Faculté des Sciences de Sfax, p. 180.

HAMED Y., DASSI L., AHMADI R., DHIA H.B., 2008, *Geochemical and Isotopic Study of the Multilayer Aquifer System in the Moulares–Redayef Basin, Southern Tunisia*. *Etude Géochimique et Isotopique du Système Aquifère Multicouche du Bassin de Moulares–Redayef, Sud Tunisien*, Hydrol. Sci. J., 53 (6), 1241–1252.

HAMED Y., BEN DHIA H., 2010, *Étude Géochimique et Isotopique de la Nappe Phréatique de la Plaine du Kef (Nord-Ouest Tunisien)*, Sécherèsse, 21 (2), 121–130.

HAMED Y., DHAHRI F., 2013, *Hydro-Geochemical and Isotopic Composition of Groundwater, with Emphasis on Sources of Salinity, in the Aquifer System in Northwestern Tunisia*, J. Afr. Earth Sci., 83, 10–24.

HAMED Y., AHMADI R., DEMDOUM A., BOURI S., GARGOURI I., BEN DHIA H., Al GAMAL S., LAOUAR R., CHOURA A., 2014, *Use of Geochemical, Isotopic, and Age Tracer Data to Develop Models of Groundwater Flow: A Case Study of Gafsa Mining Basin – Southern Tunisia*, J. Afr. Earth Sci., 100, 418–436.

HAMED Y., REDHAOUNIA B., SÂAD A.B., HADJI R., ZAHRI F., ZIGHMI K., 2017, *Hydrothermal Waters from Karst Aquifer: Case Study of the Trozza Basin (Central Tunisia)*, J. Tethys, 5 (1), 33–44.

HAMED Y., REDHAOUNIA B., BEN SÂAD A., HADJI R., ZAHRI F., 2017b, *Groundwater Inrush Caused by the Fault Reactivation and the Climate Impact in the Mining Gafsa Basin (Southwestern Tunisia)*, J. Tethys, 5 (2), 154–164.

HAMED Y., 2017, *Projet Pilote: Nouvelle Tunisie "Apport d'Eau de Mer du Golfe de Gabès a Gafsa: As Pects Socio-Economiques et Exploitation"*, [In] The 1st International Symposium (WREIANA 2017), Gafsa.

HAMED Y., BOUGUERRA W., LIMAM E., 2018a, *Projet Pilote "Transfert d'Eau de Mer du Golfe de Gabès a Gafsa: Aspects Socio-Economiques et Exploitation"*, Tunis, 2 Mars 2018, ANPR-Tunisie.

HAMED Y., HADJI R., REDHAOUNIA B., ZIGHMI K., BÂALI F., EL GAYAR A., 2018b, *Climate impact on surface and groundwater in North Africa: a global synthesis of findings and recommendation*, Euro-Mediterranean J. Environ. Integr., https://doi.org/10.1007/s4120 7-018-0063-z.

HAMMOURI M., FOHTUNG E., VASILIEV I., 2016, *Ab Initio Study of Magnetoelectric Coupling in La0.66Sr0.33mno3/Pbzr0.2Ti0.8O3 Multiferroic Heterostructures*, J. Phys. Condens. Matter., 28 (39), 396004.

IF, 1972, Bulletin of Engineering Geology and the Environment.

JING L., LI J., MASSIMO M., YUPING Y., CHAOLEI Z., JIE Z., 2018, *Performance of the Standardized Precipitation Index Based on the TMPA and CMORPH Precipitation Products for Drought Monitoring in China.*

KETROUCI K., 2002, *La Sécheresse Dans le Nord-Ouest Algérien et Son Incidence Sur la Production de Blé Dur*, Mémoire de Magister, C.U. Mascara.

KEYANTASH J., DRACUP J.A., 2004, *An Aggregate Drought Index: Assessing Drought Severity Based on Fluctuations in the Hydrologic Cycle and Surface Water Storage*, Water Resour.

KHALDI A., 2005, *Impacts de la Sécheresse Sur le Régime des Ecoulements Souterrains Dans les Massifs Calcaires de l'Ouest Algérien*, Monts de Tlemcen – Saida.

KOGAN F.N., 1990, *Remote Sensing of Weather Impacts on Vegetation in Non-Homogeneous Areas*, Int. J. Remote Sens., 11 (8), 1405–1419.

KOGAN F.N., 1995, *Application of Vegetation Index and Brightness Temperature for Drought Detection*, Adv. Space Res., 15, 91–100.

KOGAN F.N., 1995, *Droughts of Late 1980s in the United States as Derived from NOAA Polar-Orbiting Satellite Data*, National Oceanic and Atmospheric Administration.

KOGAN F.N., 1997, *Global Drought Watch from Space*, Bulletin of the American Meteorological Society, 7 (4), 621−636.

KOGAN F.N., 2002, *World Droughts in the New Millennium from AVHRR-Based Vegetation Health Indices*, Eos Trans. Am. Geophy. Union, 83 (48), 562–563.

KOGAN F., GITELSON A., ZAKARIN E., SPIVAK L., LEBED L., 2003, *AVHRR-Based Spectral Vegetation Index for Quantitative Assessment of Vegetation State and Productivity*, Photogramm. Eng. Remote Sens., 69, 899–906.

KOGAN F., STARK R., GITELSON A., JARGALSAIKHAN L., DUGRAJAV C., TSOOJ S., 2004, *Derivation of Pasture Biomass in Mongolia from AVHRR-based Vegetation Health Indices*, International Journal of Remote Sensing.

KOGAN F., YANG B., GUO W., PEI Z., JIAO X., 2005, *Modelling Corn Production in China Using AVHRR-Based Vegetation Health Indices*, International Journal of Remote Sensing, 2.

LYON JG., YUAN D., LUNETTA R.S., 1998, *A Change Detection Experiment Using Vegetation Indices*, Photogramm. Eng. Rem. Sens., 64 (2), 143–150.

MCKEE T.B., DOESKEN N.J., KLEIST J., 1993, *The Relationship of Drought Frequency and Duration to Time Scales*. [In] Proceedings of The 8th Conference on Applied Climatology, American Meteorological Society, Boston, MA., US., Vol. 17, pp. 179–183.

MCKEE T.B., DOESKEN N.J., KLEIST J., 1995, *Drought Monitoring with Multiple Time Scales*. [In] Proceedings of The Ninth Conference on Applied Climatology, Am. Meteorol. Soc., Boston, pp. 233–236.

MICHAEL HAYES., 2007, *Drought Indices 2007*, Climate Impacts Specialist, National Drought Mitigation Center.

OMM, L'Organisation Météorologique Mondiale.

PALMER W.C., 1968, *Keeping Track of Crop Moisture Conditions, Nationwide: The New Crop Moisture Index*, Weatherwise, 21, 156–161.

PALMER W.C., 1965, *Meteorological Drought*, Research Paper No. 45, U.S. Department of Commerce-weather Bureau,Washington, DC.

PALMER D.S., 1965, *Sequencing Jobs Through a Multi-Stage Process in the Minimum Total Time – A Quick Method of Obtaining a Near Optimum*, Journal of the Operational Research Society, Vol. 16, No. 1, pp. 101–107.

RADHOUANE L., 2013, *Climate Change Impacts on North African Countries and on Some Tunisian Economic Sectors*, J. Agri. Environ Intern. Dev. (JAEID), 107 (1), 101–113.

RAVI S., NITIN B., VIVEK M., 2015, *Drought Index Computation Using Standardized Precipitation Index (SPI) Method for Surat District, Gujarat.*

ROJAS O., VRIELING A., REMBOLD F., 2011, *Assessing Drought Probability for Agricultural Areas in Africa with Coarse Resolution Remote Sensing Imagery*, Remote Sensing of Environmental, 115, 343–352.

SABRI A.F., MEDJERAB A., 2012, *Evaluation de la Vulnérabilité des Bassins Versants Algériens Aux Effets des Changements Climatiques et Formulation de Stratégies d'Adaptation*, Doctoral Dissertation).

SEILER R.A., KOGAN F., GUO W.E., 2000, *Monitoring Weather Impact and Crop Yield from NOAA AVHRR Data in Argentina*, Published by Elsevier Science, Ltd., All Rights Reserve.

SEILER R.A., KOGAN F., GUO W., VINOCUR M., 2007, *Seasonal and Interannual Responses of the Vegetation and Production of Crops in Cordoba, Argentina Assessed by AVHRR-Derived Vegetation Indices*, Advances in Space Research, 39 (1), 88−94.

SERGIO M., SERRANO V., CABELL O., TOMÁS-BURGUERA T., MARTÍN-HERNÁNDEZ N., BEGUERÍA S., AZORIN-MOLINA M., EL KENAWY A., 2015, *Drought Variability and Land Degradation in Semiarid Regions: Assessment Using Remote Sensing Data and Drought Indices (1982–2011).*

SHAFER B.A., DEZMAN L.E., 1982, *Development of a Surface Water Supply Index (SWSI) to Assess the Severity of Drought Conditions in Snowpack Runoff Areas*. [In] Proceedings of The Western Snow Conference, Fort Collins, CO, pp. 164–175.

TUCKER C.J., VANPRAET C., BOERWINKEL E., GASTON EA., 1983, *Satellite Remote Sensing of Total Dry Matter Production in the Senegalese Sahel*, Remote Sens. Environ., 13, 461–47.

UNGANAI L., KOGAN F., 1998, *Drought Monitoring and Corn Yield Estimation in Southern Africa from AVHRR Data*, Remote Sensing of Environment, 63, 19−232.

USGS, U.S., *Geological Survey. Landsat 8 (L8) Operational Land Imager (OLI) and Thermal Infrared Sensor (TIRS): Calibration Notices*, available online: http://Landsat.Usgs.Gov/Calibration_ Notices.Php (accessed on 15 June 2015).

WILHITE D.A., 2005, *Drought and Water Crises: Science, Technology, and Management Issues*, CRC Press, Boca Raton, FL, USA.

WMO, World Meteorological Organization.

WU D., QU J.J., HAO X., XIONG J., 2013, *The 2012 Agricultural Drought Assessment in Nebraska Using MODIS Satellite Data*. 2013 Second International Conference on Agro-Geoinformatics (Agro-Geoinformatics), Fairfax, VA, USA, 12–16 August, pp. 170–175.